https://doi.org/10.5194/hess-2023-63
Preprint. Discussion started: 11 April 2023

Hydrology and Earth System Sciences
Discussions

An advanced tool integrating failure and sensitivity analysis to novel modeling for stormwater flooding volume

Francesco Fatone[1], Bartosz Szeląg[2], Przemysław Kowal[3], Arthur McGarity[4], Adam Kiczko[5], Grzegorz Wałek[6], Ewa Wojciechowska[3], Michał Stachura[7], Nicolas Caradot[8]

[1] Department of Science and Engineering of Materials, Environment and Urban Planning-SIMAU, Polytechnic University of Marche Ancona, 60121 Ancona, Italy
[2] Faculty of Environmental, Geomatic and Energy Engineering, Kielce University of Technology, 25-314 Kielce, Poland
[3] Faculty of Civil and Environmental Engineering, Gdansk University of Technology, 80-233, Gdansk, Poland
[4] Department of Engineering, Swarthmore College, 500 College Ave., Swarthmore, PA, 19081, United States
[5] Institute of Environmental Engineering, Warsaw University of Life Sciences-SGGW, 02-797 Warsaw, Poland
[6] Institute of Geography and Environmental Sciences, Jan Kochanowski University in Kielce, 25 – 406, Kielce, Poland
[7] Faculty of Law and Social Sciences, Jan Kochanowski University, 25 – 406, Kielce, Poland
[8] Berlin Competence for Water, Cicerostr. 24, 10709 Berlin, Germany

Correspondence to: Bartosz Szeląg (bszelag@tu.kielce.pl)

Abstract. An innovative tool for modelling specific flood volume was presented, which can be applied to assess the need for stormwater network modernisation as well as for advanced flood risk assessment. Field measurements for a catchment area in Kielce, Poland were used to apply the model and demonstrate its usefulness. This model extends the capabilities of recently developed statistical and/or machine learning hydrodynamic models developed from multiple runs of the U.S. EPA's Storm Water Management Model (SWMM) model. The extensions enable inclusion of: 1) characteristics of the catchment, and its stormwater network, calibrated model parameters expressing catchment retention and the capacity of the sewer system, (2) extended sensitivity analysis and (3) risk analysis. Sensitivity coefficients of calibrated model parameters include correction coefficients for percentage area, flow path, depth of storage, impervious area, Manning roughness coefficients for impervious areas, and Manning roughness coefficients for sewer channels. Sensitivity coefficients were determined with regard to rainfall intensity and characteristics of the catchment and stormwater network. Extended sensitivity analysis enabled an evaluation of the variability of the specific flood volume and sensitivity coefficients within a catchment, in order to identify the most vulnerable areas threatened by flooding, Thus, the model can be used to identify areas particularly susceptible to stormwater network failure and the sections of the network where corrective actions should be taken to reduce the probability of system failure. The developed simulator to determine a specific flood volume represents an alternative approach to the SWMM model that, unlike current approaches, is calibratable with limited topological data availability, therefore generates a lower cost due to the less amount and specificity of data required.

https://doi.org/10.5194/hess-2023-63
Preprint. Discussion started: 11 April 2023

Hydrology and Earth System Sciences
Discussions

Highlight

- simulator of a specific volume of flood as an alternative to the SWMM model,
- sensitivity analysis extension considering rainfall and catchment topological data,
- the probability of failure of the stormwater system as a criterion for corrective actions under conditions of uncertainty

1 Introduction

Climate change and urbanization are the main factors increasing the pressure on the functioning of sewer networks, in particular components responsible for stormwater management (Miller et al., 2014; Hettiarachchi, et al, 2018; Khan et al, 2022). This results in an increase in the frequency and volume of stormwater flooding, deterioration of the living standards of the inhabitants, and pipes abrasion (Jiang et al., 2018; Zhou et al. 2018; Chang et al. 2020). The literature data (Siekmann et al. 2011) shows that the basis for making decisions on corrective actions (replacement of a pipe, removal of sediments, construction of a reservoir, etc.) is the specific flood volume expressing the volume of stormwater flooding on a unit impervious surface. Limiting values for the specific flood volume have been determined by Siekmann and Pinnekamp (2011), based on simulations for urban catchments, as the basis for the maintenance of the sewage network and the criterion for making decisions on modernization or corrective actions.

In order to obtain a required hydraulic efficiencies, simulation models are typically used to plan corrective actions (Kirshen et al. 2014). For this purpose, mechanistic models are used, such as the USEPA's Storm Water Management Model (SWMM), which account for surface runoff, drainage of the sewage network, and flooding of stormwater during system overload (Guo et al. 2021; Li et al. 2022; Yang et al., 2022). As in the case with other mechanistic models (MOUSE, PCSWMM, MIKE URBAN etc.), SWMM can incorporate the spatial characteristics of a sewage network, as well hydraulic conditions, in calculations that predict and characterize stormwater flooding (Martins et al. 2018; Yang et al., 2020; Ma et al., 2022). However, such models are characterized by high specificity (one model can be used for one catchment), and they require the collection of detailed data and measurements (rainfall, runoff), which is labour-intensive and generates high costs. Moreover, there are a strong interactions between the calibrated parameters (Wu et al. 2013; Chen et al. 2018; Sonavane et al. 2020; Shrestha et al., 2022), leading to uncertainty of simulation results (Ball 2020; Kobarfard et al. 2022; Sun et al. 2022) which complicates to select specified corrective action (Kim et al. 2017; Bobovic et al. 2018; Hung and Hobbs 2018). To solve this problem, an important step in the development of the computational algorithm is the implementation of sensitivity analysis (Fraga et. al. 2016; Cristiano et al. 2019; Razavi and Gupta 2019). Simulations by Szeląg et al. (2021) have shown the influence of uncertainty in calibrated SWMM parameters on the calculation of specific flood volume and degree of flooding, which was also confirmed by the simulations of Fraga et al. (2016) and Kelleher et al. (2017).

To overcome the limitations of MCM, the implementation of statistical and/or machine learning methods seems is a prospective alternative (Rosenzweig et al. 2021; Lei et al. 2021; Bui et al. 2019; Shafizadeh-Moghadam et al. 2018; Chen et al. 2019; Fong and Chui, 2020). ML methods can estimate of specific stormwater flood volume for a catchment area with different topology. However, so far, no simulator model based on statistical and/or machine learning has been developed to

https://doi.org/10.5194/hess-2023-63
Preprint. Discussion started: 11 April 2023


Hydrology and Earth System Sciences
Discussions

simulate specific stormwater flood volume while taking into account the factors included in mechanistic models (Mignot et al., 2019; Guo et al. 2021; Rosenzweig et al. 2021). Some progress in application of machine learning methods to simulation of stormwater flooding has been made. Thorndahl et al. (2008), based on simulation results of flooding from manholes, including uncertainty of calibrated parameters, developed a model using the FORM (first order reliability model) method. Jato-Espino et al. (2018) and Li and Willems (2020), conducting simulations with mechanistic models, present models (logisitc regression) for identification of flooding from a single manhole based on rainfall frequency, catchment and stormwater network characteristics. Therefore, Szeląg et al. (2022a, 2022b) proposed a models for calculating estimates of stormwater flooding in a catchment, but due to insufficient data in constructing the model, application is limited. In the aforementioned models, interactions between land use, catchment and stormwater network characteristics, as well as system capacity were neglected. However, by omitting these factors, at the spatial planning stage, reduces the applicability of the model.

Another important indicator of proper sewage network management is the assessment of the risk of system failure (exceed the maximum specific flood volume). Reliable risk assessment requires the integration of mechanistic models, statistical approach and simulators of rainfall data (Fu et al. 2012; Zhou et al. 2019; Venvik et al. 2020). Most of the methods (Ursino 2014; Cea and Costabile 2022; Taromideh et al. 2022) focus on determining the impact of climatic changes in rainfall on the efficiency of the sewage system and include the impact of parameters expressing terrain and sewer retention. Currently, there is no effective method of risk analysis taking into account the uncertainty of the calibrated parameters to simulate a specific flood volume for the different urban catchments.

The aim of the article was to develop an innovated simulator, combined with risk assessment and sensitivity analyses for calculating the specific flood volume, taking into account rainfall data, catchment characteristics and topology. Recognition of the above factors enabled the application of the proposed logistic regression model to identify stormwater flooding in catchments with different characteristics, as an alternative approach to the SWMM model. An important aspect of the proposed approach was the risk assessment of system failure (specific volume of flood exceed 13 $m^3 \cdot ha^{-1}$) and sewage system operation under uncertainty. Moreover, the methodology presented in the work, integrated with the stormwater flooding simulator, enabled the identification of the impact of calibrated SWMM parameters on the results of the sensitivity analysis in catchments with different characteristics. This feature enables building a mechanistic model, which allows appropriate selection of techniques for measuring input data, which can ultimately reduce the costs of applying the model. The developed methodology enables the appropriate selection of devices for measuring the flow rate, and their location in the sewage network in the context of calibrating the catchment model and reducing the costs of flow measurements.

2 Case study

The analysed urban catchment is located in the south-eastern part of Kielce, central Poland, Świętokrzyskie region (Fig.1). Residential districts, public buildings, main and side streets are located in the study area. The catchment area covers 63 ha and consists of 40% impervious and 60% permeable areas. The road density is 108 $m \cdot ha^{-1}$ (Wałek, 2019), and the terrain denivelation is 11.20m (the ordinates of the highest and the lowest points of the terrain are 271.20 m and 260 m above sea

https://doi.org/10.5194/hess-2023-63
Preprint. Discussion started: 11 April 2023

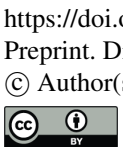

Hydrology and Earth System Sciences
Discussions

level, respectively). The length of the main interceptor channel in the stormwater network is 1569 m, with an average slope of 0.71%. The diameter of the main interceptor expands from 600 to 1250 mm, while the diameters of side sewers vary between 300 and 1000 mm. The slope of the sewers varies between 0.04 and 3.90%.

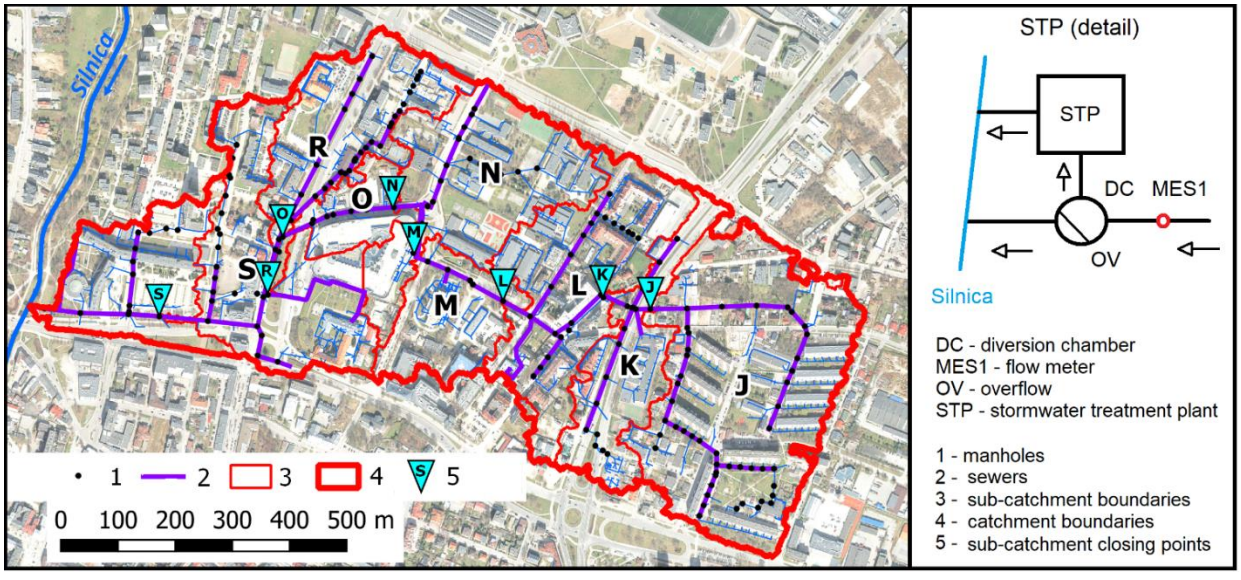

Figure. 1. Study catchment area (Wałek, 2019).

The analysed stormwater system is separated from the municipal sewage. Stormwater flows to the division chamber (DC), and after reaching a depth of 0.42 m it flows into a stormwater treatment plant (STP). During heavy rainfall, when the stormwater level in the DC exceeds the overflow level (OV), it is discharged by the storm overflow (OV) into the S1 channel, which transports the stormwater directly to the Silnica river (without treatment). At a 3.0 m distance from the inlet of the main interceptor to the DC, the flow meter MES1 is installed, which measures the flow rates during heavy rainfall with resolution of 1 minute. Analysis of data from 2010–2020 showed that during dry periods the measured flow rates varied between 1–9 $dm^3 \cdot s^{-1}$, which indicates that infiltration occurs in the stormwater network. Measurements of stormwater network operation carried out in the years 2008–2019 indicated that stormwater flooding occurs in the analysed catchment. Taking into account, 159 episodes of rainfall – runoff, within four catchments, 23 cases of flooding were observed. At a distance of 2.5 km from the catchment boundary, a rainfall measurement station is located, which provides constant measurement of rainfall, with a 1-minute temporal resolution.

Sub-catchment division and characteristics

The analysed catchment was divided into sub-catchments (Szeląg et al. 2022), which constituted study areas for identification of stormwater flooding. Due to limited amount range of rainfall data, the obtained model for simulation of stormwater overflow did not include all important factors, such as dry period duration between rainfall events, retention

https://doi.org/10.5194/hess-2023-63
Preprint. Discussion started: 11 April 2023

Hydrology and Earth System Sciences
Discussions

catchment that impact flooding phenomenon, which meant that the model had limited predictive capability. Detailed description and justification of sub-catchments used for construction of flooding identification model was presented by Szeląg et al. (2022). In reference to approach proposed by Duncan et al. (2011), Jato – Espino et al. (2018), Li and Willems (2022), in the current analysis the number of sub-catchments used for development of a logit model was increased to 8 (Figure 2). The sub-catchments boundaries together with data on spatial development and stormwater network (Table 1) were determined based on maps for design purposes, which was discussed in detail by Szeląg (2013).

Table. 1. Characteristics of sub-catchments

No.	F	Imp	Vk	Gk	R.t.	Vkp	dH1	dHp	Lk	Jkp	Hst	Impd	Gkd	Vrd	Vkd
	ha	-	m^3	$m \cdot ha^{-1}$	m	m^3	m	m	m	-	m	-	$m \cdot ha^{-1}$	m^3	m^3
J	12.66	0.37	157.0	0.0079	1.74	33.2	0.24	0.25	96.5	0.0036	1.42	0.40	0.0072	2159.4	2577.2
K	18.92	0.38	360.4	0.0084	1.69	28.4	0.31	1.05	56.5	0.0055	2.36	0.40	0.0063	1886.8	2373.7
L	27.15	0.36	557.4	0.0074	2.74	29.6	0.34	1.75	59.0	0.0058	2.36	0.42	0.0053	1496.0	2176.7
M	29.78	0.36	678.8	0.0068	4.49	48.7	0.38	1.15	62.0	0.0061	2.32	0.43	0.0050	1373.3	2055.3
N	36.78	0.37	712.2	0.0081	4.49	48.7	0.38	1.15	62.0	0.0061	2.32	0.44	0.0040	1061.4	2022.0
O	41.31	0.32	858.2	0.0079	5.32	16.1	0.21	1.28	20.5	0.0102	2.31	0.49	0.0037	825.9	1876.0
P	45.42	0.37	981.9	0.0082	5.64	16.1	0.21	1.28	20.5	0.0102	2.31	0.46	0.0027	682.2	1752.3
R	48.31	0.37	981.9	0.0088	5.64	16.1	0.21	1.28	20.5	0.0102	2.31	0.47	0.0023	553.1	1752.3
S	55.41	0.41	1240.2	0.0092	8.47	67.5	0.67	1.8	86.0	0.0078	2.31	0.55	0.0011	258.4	1493.9

where: F – catchment surface area; Imp – impervious area; Vk – volume of stormwater channel; Gk – length of stormwater channel per impervious area of the catchment; R.t. – height difference of the channel, Vkp – volume of the channel above the cross-section of a catchment; dH1 – height difference of the terrain at section above cross-section r; dHp – height difference at section above cross-section; Lk – length of channel above cross-section of a catchment; Jkp – channel slope above cross-section of a catchment; Hst – the height of a manhole at cross-section; Imp – impervious area of downstream area; Gkd – length of a channel per impervious area below cross-section; Vrd – catchment retention above the cross-section calculated as $Vrd = F \cdot (Imp \cdot d_{imp} + (1-Imp) \cdot d_{per})$, Vkd – total retention of a catchment.

Data were verified using independent analysis performed by Wałek (2019), who used Qgis program to develop spatial development model and stormwater network for Kielce. Location of closing cross-sections of sub-catchments (J, K, L, M, M, O, P, R, S) along the main interceptor were additionally supported by simulation results of outflow hydrographs developed by Wałek (2019) with use of HEC-HSM model as well as by Szeląg et al. (2014, 2022) with use of hydrodynamic model SWMM.

3 Methodology

3.1. Criterion for stormwater system operation and modernisation

https://doi.org/10.5194/hess-2023-63
Preprint. Discussion started: 11 April 2023


Hydrology and Earth System Sciences
Discussions

The value of a specific flood volume was defined as stormwater flooding per unit impervious area, which can be expressed by the following formula (Sinekamp and Pinekamp, 2011):

$$\kappa = \frac{\sum_{i=1}^{K} V_{t(i)}}{A_{imp}} \quad (1)$$

where: V_t – volume of stormwater flooding from i-th manhole of the stormwater network, K – number of manholes, A_{imp} – impervious area. Sinekamp and Pinekamp (2011) based on continuous simulations with hydrodynamic models for 3 urban catchments found that the specific flood volume ranged from 0 - (>20) $m^3 \cdot ha^{-1}$.

On this basis, they established limiting κ values expressing the need to improve the operating conditions of the drainage system. They showed that for $\kappa > 13$ $m^3 \cdot ha^{-1}$ the drainage system requires adaptation This was also confirmed by the calculations of Kotowski et al. (2014) for the catchment in Wroclaw and Szeląg et al. (2021) for the catchment in Kielce. This allows us to conclude for urban catchments (Poland, Germany) that the κ value quoted above can be a criterion for making decisions on corrective actions of the drainage network.

3.2. Simulator structure and development

The concept of the proposed of tool based on simulator integrated with the risk assessment and sensitivity analysis to evaluate operation of sewage system was presented in Fig. 2.Applying the MCM of an urban catchment with separate sub-catchments (varying land use and topology), a simulator of the specific flood volume was developed as an alternative approach to the SWMM. A proposed simulator of logistic regression model-based on rainfall data, catchment and stormwater network characteristics, SWMM parameters (width of runoff path, retention depth of impervious areas, Manning roughness coefficient of impervious areas, correction coefficient of impervious areas, Manning roughness coefficient of channels). The resulting tool enables fast analysis of sewer network performance even with limited data access and can be applied to other catchments. Proposed methodology is based on extension of algorithms given by Szeląg et al. (2021, 2022). In contrast to previous studies (Szeląg et al. 2022), the current approach took into account the retention of the catchment and the sewer network, and the performance criterion of the sewer network was the volume of flooding and not just the fact that it occurred. Integration of the simulator with an analytical relationship for sensitivity coefficient calculations for logistic regression allows fast evaluation of the impact of MCM parameters on flooding for arbitrary catchment characteristics and topological data. In order to provide more reliable simulation results, the proposed risk assessment took into account the uncertainty of the SWMM parameters and enabled the optimisation of the operation of the sewer network based on the maximum allowable values of the channel Manning roughness coefficients.

https://doi.org/10.5194/hess-2023-63
Preprint. Discussion started: 11 April 2023

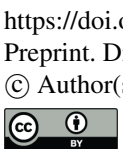

Hydrology and Earth System Sciences
Discussions

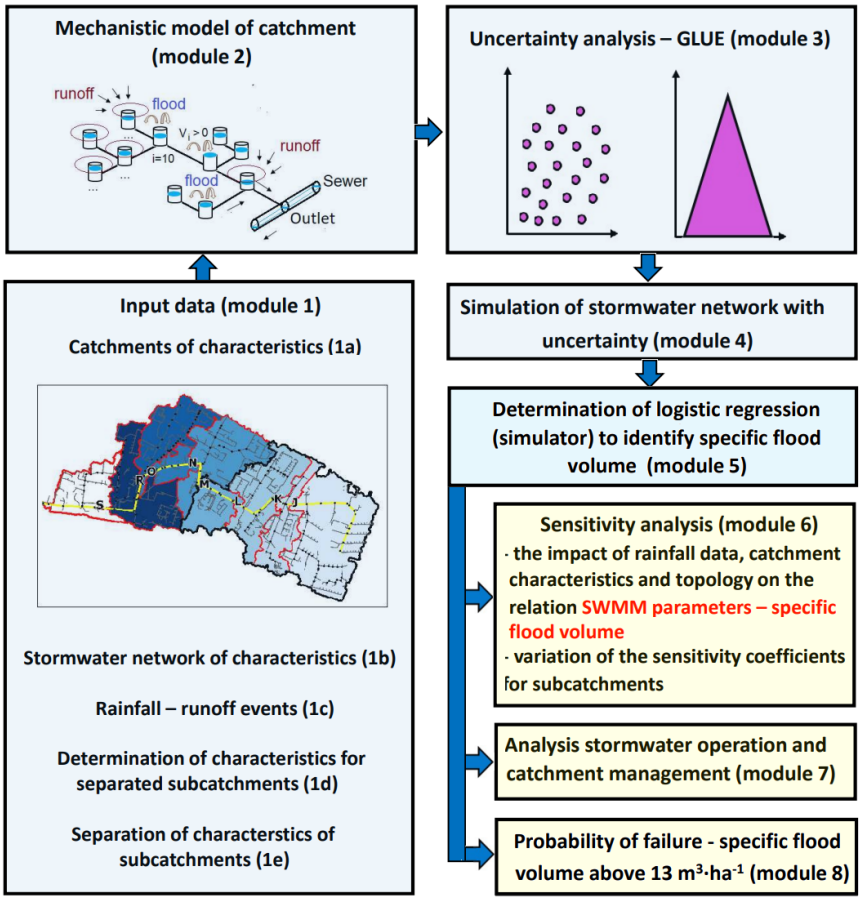

Figure. 2. Algorithm for developing an advanced tool to simulate a specific flood volume (situation maps in module (1a), (1b) by Walek (2019).

3.3. Algorithm structure

The proposed computation algorithm consists of 9 modules. Modules 1, 2, 3, 4 include identical steps as in the work of Szeląg et al. (2021, 2022). In the present study, the scope of the analyses was extended, as in addition to precipitation data and SWMM parameters (Szeląg et al. 2022), the characteristics of the catchment and the stormwater network of the separated sub-catchments were also included (module 1), which was used to determine the computational model. On the basis of spatial data (1a, 1b), a mechanistic model of the catchment was built (module 2), which allowed to perform an uncertainty analysis using the GLUE method (module 3). On this basis, simulations were performed in separated sub-catchments for rainfall events (1e) under uncertainty (module 4). Based on the simulation results a logistic regression model was developed (module 5) to calculate the local sensitivity coefficients for calibrated SWMM parameters, with regard to rainfall intensity and catchment characteristics (module 6). Modules 1, 2, 3, 4 included analyses to determine a specific flood volume simulator that can be applied to any catchment. Thus, future algorithm implementation for the new catchment, will ultimately include only modules

https://doi.org/10.5194/hess-2023-63
Preprint. Discussion started: 11 April 2023


Hydrology and Earth System Sciences
Discussions

6, 7, 8. Using adopted rainfall data, the sensitivity coefficients of SWMM model parameters for sub-catchments are computed and maps showing sensitivity changes in catchment scale are drawn (module 6). While the model is applied to identify stormwater flooding, the possible methods for improving stormwater network operating are analysed inside module 7, 8. Computations using the developed algorithm consist of the following steps:

1) collecting of the input data (catchment characteristics – 1a, stormwater network characteristics – 1b, rainfall – runoff episodes – 1c), separation of independent rainfall episodes – 1d, division and determination of characteristic of sub-catchments – 1e,

2) development of hydrodynamic model (module 2) based on catchment characteristics (1a) and stormwater network characteristics (1b),

3) conducting of uncertainty analysis with GLUE method (section 3.3.3) using hydrodynamic model of a catchment based on rainfall – runoff episodes (1d),

4) using independent rainfall events (1d) simulations with hydrodynamic model including uncertainty of calibrated parameters according to points (4a, 4b, 4c) are conducted;

a) simulation of SWMM parameters (*a posteriori distribution*) in Table S1 using the results of uncertainty analysis,

b) simulation of stormwater network operation during independent rainfall events (1d) including uncertainty (4a),

c) computation of specific flood volume in each sample of independent rainfall events in sub-catchments; transformation of determined κ values to classification data (section 4a),

5) determination of logistic regression simulator SWMM of specific flood volume as alternative to MCM model based on results of computations in point 4c,

6) sensitivity analysis:

a) computations of sensitivity coefficients (with regard to SWMM parameters) for assumed rainfall data and catchment characteristics,

b) computations of sensitivity coefficients for sub-catchments (J, K, L, M, N, O, P, R, S),

7) application of developed logistic regression model for amelioration of stormwater network operation,

a) analysis of the impact of corrective variants on sensitivity coefficients in sub-catchments,

8) analysis of failures occurrence.

3.3.1. Determination of independent rainfall events (module 1e)

Determination of independent rainfall events for the period 2010 - 2021 was based upon criteria defined in DWA A-118 (2006) guidelines. The minimum time period between independent rainfall events was set as 4.0 hours. Computation of stormwater flooding was performed for rainfall events with a minimum depth of P_t = 5.0 mm (Fu and Butler, 2014) and only for those events that resulted from convection rainfalls (i.e., rainfall duration below 120 min). For the analysed catchment, it was indicated that stormwater flooding occurs for C = 2, 3, 5 and rainfall duration t_r = 120 min (Szeląg et al., 2021). The computed values of specific flood volume (the upper limit of 95% confidence interval) are $\kappa = 45\ m^3 \cdot ha^{-1}$. Analyzing of the

https://doi.org/10.5194/hess-2023-63
Preprint. Discussion started: 11 April 2023


Hydrology and Earth System Sciences
Discussions

rainfall data, it was observed that the number of rainfall events with depths of P_t = 5.2–42 mm ranged from 12 to 30 in each year (210 rainfall events altogether), while the rainfall durations were between t_r = 15 –120 min.

3.3.2. Hydrodynamic catchment model (module 2)

Stormwater flooding volume calculations were performed with the SWMM model using the „Flooding" function (Szeląg et al. 2021). Based on the results of $Q(t)$ for j – manholes (j = 1, 2, 3 ..., k) in the sub-catchments (J, K, L, M, N, O, P, R, S), the total flooding volume $V_j = \int Q(t)dt$ was determined, which allowed specific flood volume (κ) values to be determined from Equation (1).

The model of analysed catchment covers 62 ha and is divided into 92 sub-catchments with areas varying from 0.12 to 2.10 ha and impervious areas ranging 5 to 95%. The model comprises 82 nodes and 72 sections of channels. At the calibration stage method of the „trial and error", the mean retention of the catchment equal of 4.60 mm. The Manning coefficient of impervious areas was found to be 0.025 $m^{-1/3}$·s and 0.10 $m^{-1/3}$·s for pervious areas. The flow path width was determined using the formula $W=\alpha \cdot A^{0.50}$, where: α = 1.35. Catchment model calibration performed by Szeląg et al. (2021) indicated that for 6 rainfall-runoff events, a very good fit of modelling outflow hydrographs to measurement results was obtained (Nash - Sutcliff coefficient was 0.85 - 0.98, coefficient of determination was equal to 0.85 - 0.99, hydrograph volumes and maximum flows did not exceed 5% compared to measurement data).

3.3.3. Uncertainty analysis – GLUE (module 3)

In the GLUE method, the identification of model parameters was considered as a probabilistic task due to the large number of parameters characterizing processes occurring in urban catchments (runoff, infiltration, flow in stormwater conduits, flooding) – Szeląg et al. (2021), Kiczko et al. (2018), Mannina et al. (2018). The identification of model parameters in the GLUE method depends on the transformation of an *a priori distribution* to an *a posteriori distribution* by means of a likelihood function $L(Q/\theta)$, which determines the probability of a combination of parameters depending on the quality of fit of the calculation result to the measured values. Uniform distribution of SWMM parameters was assumed (Table S1). Mathematical models used for description of surface runoff usually do not include runoff distribution and at most they include the range of admissible values of parameters resulting from their physical interpretation (Dotto et al., 2014; Knighton et al., 2016). Identification of distributions *a posteriori* and determination of likelihood functions the rainfall - runoff episodes 30 May 2010 and 8 July 2011 were used, while for verification the episodes from 15 September 2010 and 30 July 2010 were applied. Subsequent computation steps of GLUE analysis were discussed in detail in Supplementary Information (Section 1).

3.3.4. Simulation of stormwater network operating with regards to uncertainty (module 4)

Based on the results of GLUE (*a posteriori distribution* SWMM parameters, 5000 sampling), the computation of stormwater network was performed for separate 175 independent rainfall events and 9 subcatchments; 35 events were used to validate the model. The values of specific flood volume for sub-catchments (J, K, L, M, N, O, P, R, S) were calculated and

https://doi.org/10.5194/hess-2023-63
Preprint. Discussion started: 11 April 2023


Hydrology and Earth System Sciences
Discussions

zero-one variables were established to develop logistic regression model. For computed values of specific flood volume ($\kappa \geq$ 13 $m^3 \cdot ha^{-1}$) the variable value was denoted as 1, while in the opposite case it was 0 (Siekmann and Pinekamp, 2011).

3.3.5. Developing a logistic regression model – simulator specific flood volume (module 5)

Logistic regression model (LRM) is a tool used for classification. This model has been already applied for modelling stormwater flooding (Szeląg et al., 2020), identifying stormwater flooding from manholes (Jato – Espino et al., 2018) and the technical condition of sewage systems (Salman and Salem, 2012). The logistic regression model is described by the following equation:

$$p_m = \frac{\exp(\alpha_0+\alpha_1 \cdot x_1+\alpha_2 \cdot x_2+\alpha_3 \cdot x_3+\cdots+\alpha_i \cdot x_i)}{1+\exp(\alpha_0+\alpha_1 \cdot x_1+\alpha_2 \cdot x_2+\alpha_3 \cdot x_3+\cdots+\alpha_i \cdot x_i)} = \frac{\exp(X)}{1+\exp(X)} = \frac{exp(X_{rain}+X_{SWMM}+X_{Catchm})}{1+exp(X_{rain}+X_{SWMM}+X_{Catchm})} \quad (2)$$

where p_m – probability of a specific flood volume (understood as the need to corrective actions the stormwater network); α_0 – absolute term; α_1, α_2, α_3, α_i – values of coefficients estimated with the maximum likelihood method, X – vector describing the linear combination of the independent variables; X_{rain}/ X_{SWMM}/ X_{Catchm} – vector describing linear combination of statistically significant:

(a) rainfall characteristics ($X_{rain} = \sum_{s=1}^{t} \alpha_s \cdot x_s$),

(b) SWMM parameters ($X_{SWMM} = \sum_{k=1}^{m} \alpha_k \cdot x_k$),

(c) catchment characteristics, and stormwater network characteristics confidence level – 0.05 ($X_{Catchm} = \sum_{p=1}^{r} \alpha_p \cdot x_p$); x_i – independent variables describing rainfall characteristics, e.g., rainfall depth, its duration, and the parameters calibrated in the SWMM, catchment characteristics (permeability, terrain retention, density of stormwater network, length, slope, retention in stormwater channels etc.).

Independent variables in the logit model were calculated using the forward stepwise algorithm, recommended for the creation of such models. At the same time, it also ensures the elimination of correlated independent variables (Harrell 2001). The estimation of the coefficients α_i in Equation (4) and thus the determination of the logistic regression model involved two stages: learning (80%) and testing (20%). Optimisation of the p_m threshold, equations for determining measures of fit between computational results and measurements was provided in Supplementary Information (Section 2). A validation of the obtained logistic regression was additionally performed using the SWMM model for 35 rainfall events (catchment characteristics and topological data were analysed for separated sub-catchments J, O, S within ±20%), in order to assess the extent of applicability of the obtained model.

3.3.6. Sensitivity analysis (module 6)

According to literature data (Morio, 2011), despite simplifications, local sensitivity analysis is widely applied at the calibration stage and while analysing the hydrodynamic catchment models. In our study, the sensitivity coefficient was calculated from the equation (Petersen et al. 2012):

https://doi.org/10.5194/hess-2023-63
Preprint. Discussion started: 11 April 2023


Hydrology and Earth System Sciences
Discussions

$$S_{xi} = \frac{\partial p_m}{\partial x_i} \cdot \frac{x_i}{p_m} \quad (3)$$

Where, knowing that $\frac{\partial p_m}{\partial x_i} = \beta_i \cdot p_m \cdot (1 - p_m)$, after transformations, the following formula was obtained (Fatone et al. 2021):

$$S_{xi} = \beta_i \cdot x_i \cdot (1 - p_m) \quad (4)$$

Value of the S_{xi} was calculated for calibrated SWMM parameters (Table S1), at the same time analysing the impact of rainfall duration (t_r = 30 – 90 min) for rainfall depth P_t = 10 mm (representative value for analysing stormwater network functioning according to DWA – A 118, corresponding to a heavy rainfall event). For the above assumptions, S_{xi} was determined for different catchment characteristics, which at the same time helped to evaluate the interactions between rainfall data and the parameter SWMM.

The probability of the specific flood volume (p_m) was computed using the logistic regression model for the sub – catchment characteristics defined in Table 2 and SWMM parameters established during calibration (Szeląg et al., 2016) for maximum convection rainfall intensity for t_r = 30 min and P_t = 9.62 mm for Kielce (Section 3 at Supplementary Information). The calculations of Szeląg et al. (2022) proved that in the urban catchment in question there is a hydraulic overload of the stormwater system due to convective rainfall. At the same time, the sensitivity coefficients for calibrated SWMM model parameters were calculated. On this basis the spatial variability of S_{xi} for the sub-basins was determined.

3.3.7. Application of the logit model to analyse stormwater operating and catchment management (module 8)

If the stormwater network ceases to function properly and the threshold value of p_m is exceeded, some possible improvements were suggested, including: (a) increasing the retention depth of impervious areas, i.e. an increase of d_{imp} from 2.50 mm to 3.50 mm, and at the same time raising the Manning roughness coefficient from n_{imp} = 0.025 $m^{-1/3} \cdot s$ to n_{imp} = 0.035 $m^{-1/3} \cdot s$, (b) an increase of hydraulic capacity by reducing the Manning roughness coefficient for stormwater channels from n_{sew} = 0.018 $m^{-1/3} \cdot s$ to n_{sew} = 0.012 $m^{-1/3} \cdot s$. In addition, the possible change of spatial development of urban catchment area was taken into consideration. Finally, combinations of the above-mentioned computation variants were analysed. When the values of independent variables (catchment characteristics) adopted for the calculations exceeded the lower/upper (e.g., for Imp = 0.32 - 0.41) limit of applicability of the determined logit model, the simulation results were verified with the mechanistic model. The verification procedure consisted of three steps:

a) computation of the probability of specific flood volume for rainfall with durations in the range of t_r = 30 – 90 min to assess stormwater network operating,

b) simulation with a calibrated hydrodynamic model for rainfall data as in step (a),

c) comparison of computation results obtained in steps (a), (b); in the event of a of good fit, i.e., proper identification of specific flood volume, the results obtained from the logit model can be accepted. Three specific corrective variants have been defined as presented in Table S2.

3.3.8. Probability of stormwater network failure (module 9)

https://doi.org/10.5194/hess-2023-63
Preprint. Discussion started: 11 April 2023


Hydrology and Earth System Sciences
Discussions

The probability of failure (Sun et al., 2012; Karamouz et al., 2013) was used to analyze the performance of the sewage network in a rainfall event. In the calculations, a failure was defined as an episode (assumed rainfall data, catchment characteristics, sewer network, SWMM parameters described by *a posteriori distribution* - GLUE results discussed in Section 3.3.3) in which $\kappa \geq 13 m^3 \cdot ha^{-1}$ ($p_m \geq p_{m,cr}$) is exceeded. However, the probability of failure was calculated from the equation:

$$p_F = \frac{\sum_{j=1}^{N} Z_j}{N},\ where: Z_j = \begin{cases} 1;\ p_m \geq p_{m,cr} \\ 0;\ p_m < p_{m,cr} \end{cases} \quad (5)$$

where: p_m – probability of specific flood volume (exceedance of this value indicates a failure), p_F – probability of the stormwater network failure in the event of rainfall, Z_j – function describing stormwater network operation, for $Z_j = 1$ – drainage system requires modernisation; otherwise, i.e. $Z_j = 0$ – modernisation is not necessary.

Based on Equation (5) for the assumed characteristics (rainfall, catchment, drainage network), the operating conditions of the stormwater network were determined. Hence, an algorithm is given to calculate the performance improvement of a sewer network in the context of failure probability (p_F) reduction. The above effect was obtained by introducing thresholds of maximum permissible values of Manning roughness coefficients of sewers $n_{sew(m)}$. It was assumed that if the value of nsew (the value from the *a posteriori distribution*) exceeds the maximum permissible value - $n_{sew(m)}$ and determines the occurrence of failure ($Z_j = 1$) and the need to modernize the sewers, it should be corrected in such a way that $p_m < p_{m,cr}$. The above calculations were reduced to the following steps:

a) *a posteriori distribution* of calibrated SWMM model parameters (N = 5000 samples),

b) computation of probability of specific flood volume for N items and establishment of failure probability,

c) computation of the Manning roughness coefficient for channels when $p_m > p_{m,cr}$ from the following formula:

$$n_{sew} = \frac{1}{\alpha_{nsew}} \cdot \left[ln\left(\frac{p_{m,cr}}{1-p_{m,cr}}\right) - \left(\sum_{k=1}^{m-1} \alpha_k \cdot x_k\right) - \boldsymbol{X}_{rain} - \boldsymbol{X}_{Catchm} \right] \quad (6)$$

where: k = 1, 2, 3, …, m – calibrated SWMM model parameters; k = 1, 2, 3, …, m; α_{nsew} – estimated coefficient in logistic regression model for the Manning roughness coefficient for channels (derivation of the Equation 6 was presented in the Supplementary Information – Section 4),

d) establishment of empirical distribution describing the n_{sew} values calculated from Equation (6),

e) computation of n_{sew} values from Equation (8) for $n_{sew(un)} \leq n_{sew(m)}$ (where: $n_{sew(un)}$ – Manning roughness coefficients of channels computed in step (a), $n_{sew(m)}$ – maximal boundary (threshold) value of Manning roughness coefficient for channels), when $n_{sew(un)} \geq n_{sew(m)}$ to $n_{sew} = n_{sew(un)}$,

f) computation of probability of specific flood volume and probability of failure (p_F),

g) determination of empirical distribution (CDF) for n_{sew},

h) steps e – g are repeated r = 1, 2, 3, .., z – for different values of $n_{sew,max}$ and median values of $n_{sew(0.5)} = f(n_{sew(m)}, r)$ are denoted based on empirical distributions,

i) steps a–h are conducted for different catchment characteristics,

https://doi.org/10.5194/hess-2023-63
Preprint. Discussion started: 11 April 2023

Hydrology and Earth System Sciences
Discussions

j) graph $p_F = f(n_{sew(0.5)})$ is drawn.

4. Results

4.1. Uncertainty analysis – GLUE (module 3)

Based on SWMM simulation results including uncertainty of calibrated parameters (Table S1), the likelihood functions were determined (Kiczko et al., 2018). For the observational events (30 May 2010 and 8 July 2011) used to identify the SWMM parameters, it was found that 96% of the measurement points included the calculated confidence interval. For the validation sets, 90% of the observation points fall within the bands for the 15 September 2010 event and 70% for 30 July 2010 (Figure S1). The results of the likelihood function calculations for the calibrated SWMM model parameters are given in Figures S2 – S3 in Supplementary Information.

4.2. Simulations of stormwater network operation with regard to uncertainty (module 4)

The results of variation of specific flood volume for the separated sub-catchments has been presented in Figure 3. Based on the obtained curves it was stated that the uncertainty of SWMM parameters influenced the simulation results, which was confirmed by the great variability of the 1% and 99% percentile values for each sub-catchment.

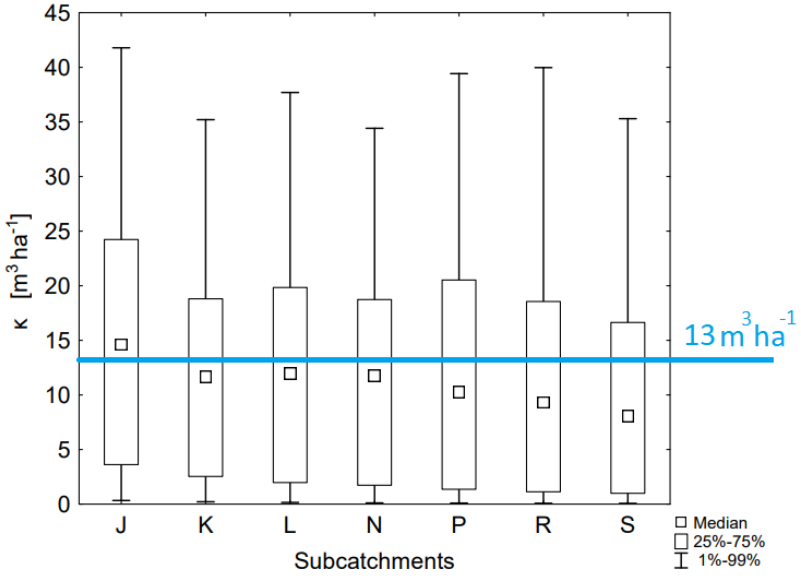

Figure. 3. Variability of specific flood volume for sub-catchments.

The median values, enabled to identify that the largest specific flood volume was for sub-catchment J (14.90 $m^3 \cdot ha^{-1}$), and 8.29 $m^3 \cdot ha^{-1}$ for the sub-catchment S (Figure 3). The simulation results for the 1% percentiles showed that for adopted rainfall events ($P_t > 5.0$mm and $t_r < 150$ min) stormwater flooding occurred in all sub-catchments. It was demonstrated that problems with operating of the

https://doi.org/10.5194/hess-2023-63
Preprint. Discussion started: 11 April 2023


Hydrology and Earth System Sciences
Discussions

stormwater network are present in each sub-catchment, since the calculated values of percentiles (75%, 99%) are higher than 13 $m^3 \cdot ha^{-1}$. This indicates that the stormwater network requires modernisation.

4.3. Determination of the logistic regression model (module 5)

A LRM was built based on the operational simulation of the stormwater network. The model can be used to identify specific flood volume and for decision-making regarding corrective actions of the stormwater system. The relationship from Equation (2) was described by the following linear combination:

$$X_{rain} = 4.05 \cdot P_{tot} - 0.18 \cdot t_r - 54.15 \quad (7)$$

$$X_{SWMM} = 0.23 \cdot \alpha - 79.40 \cdot n_{imp} + 6.23 \cdot \beta + 0.33 \cdot \gamma + 234.12 \cdot n_{sew} \quad (8)$$

$$X_{Catchm} = 76.72 \cdot Imp + 40.77 \cdot Impd - 0.01 \cdot Vk - 1967.04 \cdot Gk - 1169.00 \cdot Gkd - 20.33 \cdot Jkp \quad (9)$$

For other independent variables (Table S2) the determined coefficients were statistically insignificant in prediction confidence band 0.05. Standard deviations of the coefficients estimated from the logit model and the test probabilities are presented in Table S2. The best fit of the computed results to the measurement data was obtained for $p_{m,cr} = 0.75$. For the test data set (20%) the following values were obtained: SPEC = 95.24%, SENS = 84.62% and Acc = 87.87%.

For the determined independent variables (Equation 7, 8), calculations were performed with the LRM and SWMM model (for 35 rainfall events, $P_t \geq 5$ mm and $t_r \leq 120$ min) assuming values of catchment characteristics and topological data within ±20% in the separated sub-catchments. The simulation variants analysed and calculation results are given in Table S4 – S11. The results obtained confirm that the determined LRM model can be applied in a wider range than shown in Table 1. The maximum difference in the number of events when $\kappa > 13$ $m^3 \cdot ha^{-1}$ by the ML model and SWMM for Imp = 0.26 - 0.50, Impd = 0.32 - 0.66, Gk = 0.0068 - 0.011 $m^3 \cdot ha^{-1}$, Gkd = 0.0009 – 0.0013 $m^3 \cdot ha^{-1}$ does not exceed 4 episodes, which confirms the usefulness of the model.

4.4. Sensitivity analyses (module 6)

For rainfall depth P_{tot} = 10 mm and duration t_t = 30 – 90 min, the sensitivity coefficients for the SWMM model were determined, based on Equation (4). For calculation of S_{xi} the values established during calibration were adopted (Kiczko et al., 2018). The computation results for two parameters of the SWMM model (β and n_{imp},) are presented in Figure 4. These two parameters appeared to have the most significant impact on specific flood volume and, at the same time, they present a vastly different impact on the dynamics of changes regarding $S_{xi} = f(t_r, Imp, Impd, Vk, Jkp)$; the calculation results for the other SWMM model parameters are given in Figures S4–S8 (Supplementary Information).

The Figure 4 and Figures S4 – S8 indicated that for the adopted values of t_r and Imp, Impd, Vk, Jkp, the highest values of S_{xi} was obtained for correction coefficient percentage of impervious areas (β), Manning roughness coefficient for sewer channels (n_{sew}) and Manning roughness coefficient for impervious areas (n_{imp}). Retention depth of impervious areas (d_{imp}) had the lowest impact on the results of specific flood volume. An increase of rainfall duration results in higher values of S_β, S_{nimp}

https://doi.org/10.5194/hess-2023-63
Preprint. Discussion started: 11 April 2023

(Figure 4). The lowest sensitivity coefficients were obtained for t_r = 30 min while the highest for t_r = 90 min. An increase of Imp, Impd results in a decrease of S_β and S_{nimp} sensitivity coefficients.

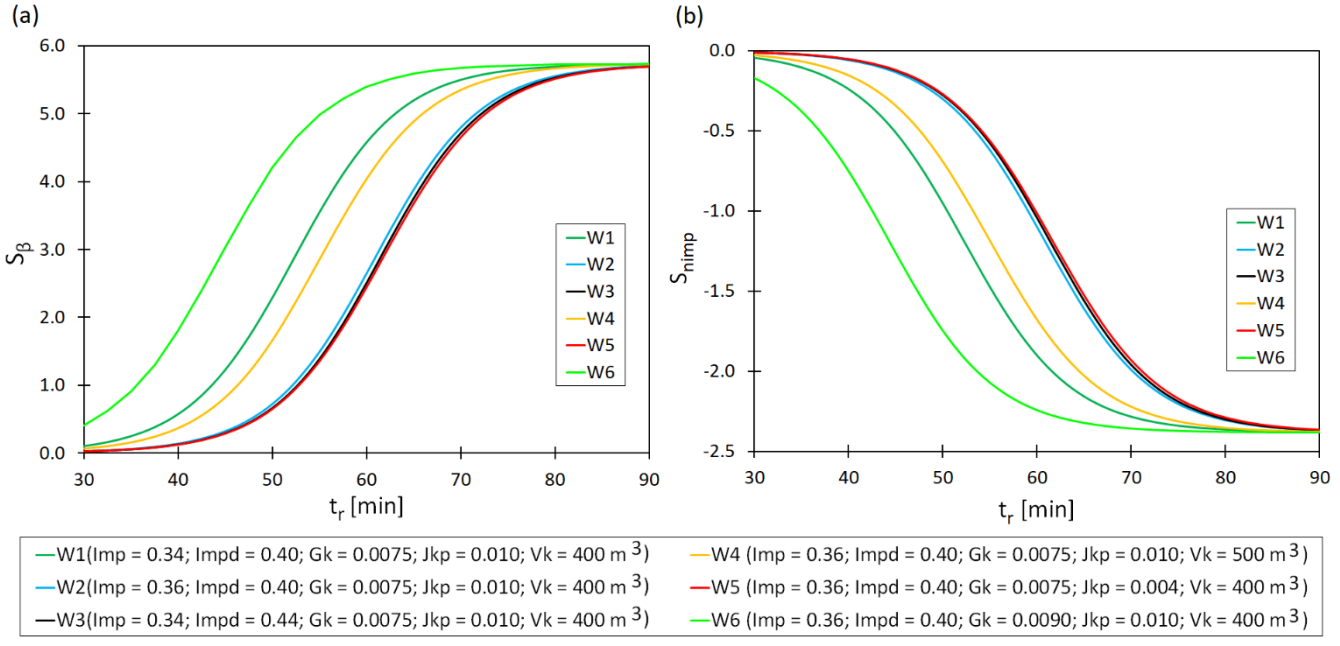

Figure 4. The impact of rainfall duration (t_r) and catchment characteristics (Imp, Impd, Vk, Jkp) on sensitivity coefficients: (a) S_β, (b) S_{nimp}.

For instance, an increase of Imp from 0.34 to 0.36 results in a decrease of S_β from 1.23 to 0.28; identical values were obtained for Impd (Figure 4). Moreover, an increase of Vk, Jkp, Gk leads to an increase of S_β and S_{nimp} sensitivity coefficients. Among analysed catchment characteristics, density of stormwater network (Gk) had the highest impact on sensitivity coefficients, while longitudinal slope of canal (Jkp) was of the lowest significance, which is confirmed by variability of obtained curves for subsequent SWMM parameters (Figure 4).For example, when Vk increased from 400m^3 to 500 m^3, S_β increased from 0.29 to 0.82. Additionally, a 10% growth of S_β was observed due to a change of Jkp = 0.004 to Jkp = 0.010. Finally, when Gk increased from 0.0075 to 0.009 S_β also increased from 0.29 to 3.03 (Figure 4).

4.6. Implementation of logit model to analyse the operating of the stormwater network and catchment management (module 7 & 8)

Due to the fact that in the analysed stormwater network an exceedance of specific flood volume was observed, possible improvements to the network were considered in terms of correcting catchment imperviousness (Imp) as well as enhanced terrain retention and channel capacity. The results of p_m computations are presented in Figure 5, while Figure 6 shows S_β for variants I, II and III for sub-catchments. Simulation results for the sensitivity coefficients of other SWMM model parameters (Table S1) and the probability of specific flood volumes are presented in Figures. S9–S17.

https://doi.org/10.5194/hess-2023-63
Preprint. Discussion started: 11 April 2023

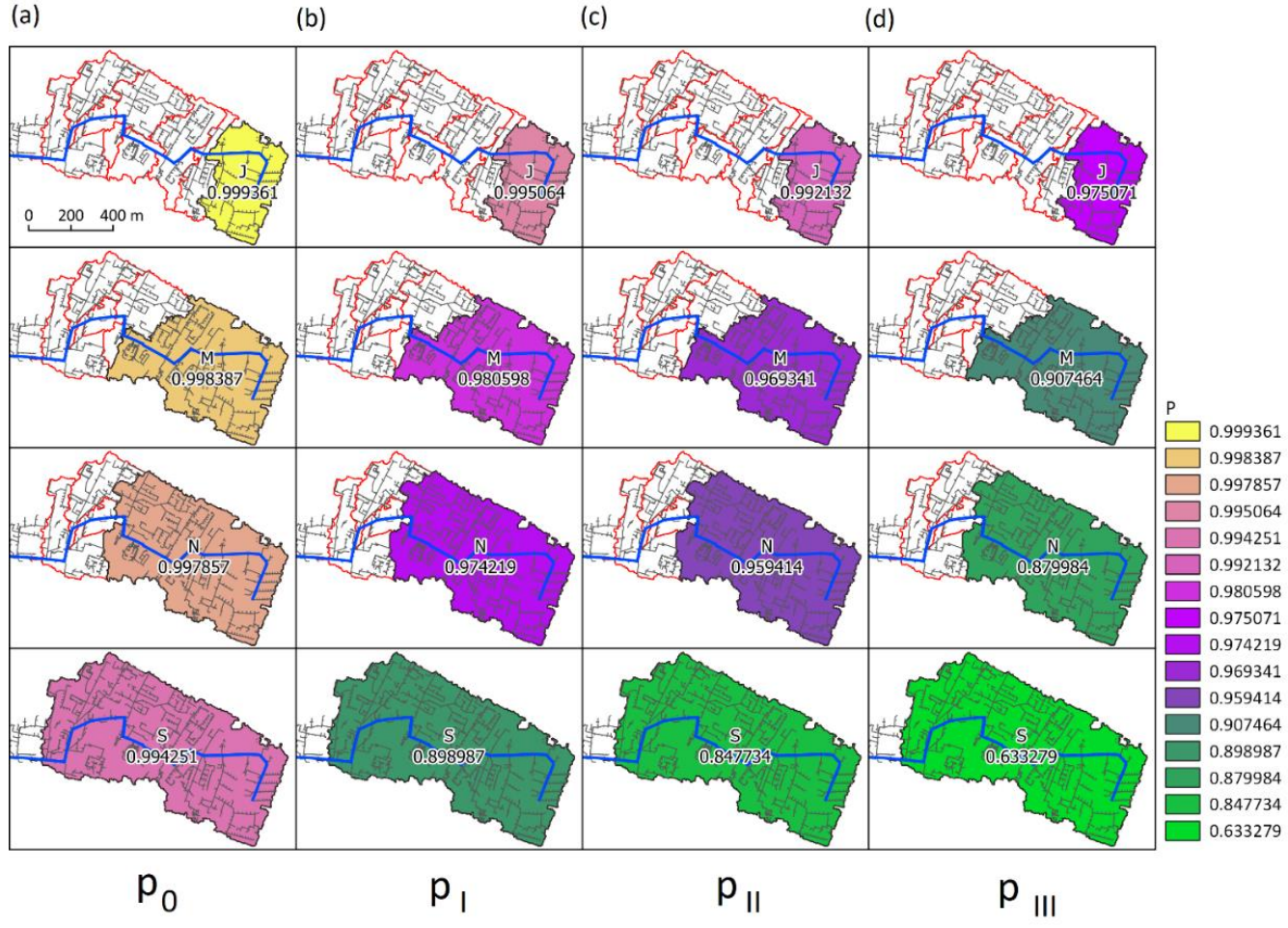

Figure 5. Probability of specific flood volume in sub-catchments for: (a) present state (p_0) and for (b) I, (c) II, (d) III corrective actions variants.

A decrease of Imp by 10% in sub-catchment J has negligible impact on p_m value, while in sub-catchment S it results in the decrease of specific flood volume probability by 10% (Figure 5a, 5b). It was found that decrease of catchment imperviousness (variant I) leads to improvement of stormwater system operation (Figure 5). The greatest reduction in volume flooding was obtained for variant III, when p_m values decreased by 2% and 36% for sub-catchments J and S (Figure 5d).

Based on the p_m values in catchments J, M, N, S for corrective action variant III, it was found that, despite the increase in retention depth, channel capacity and reduction in imperviousness of the catchments, there was hydraulic overloading ($\kappa > 13$ $m^3 \cdot ha^{-1}$) in the sub-catchments. This indicates the need for further changes to both the catchment and the stormwater network than was assumed. For variants I, III the Imp values for the sub-catchment are below the applicability range of the logit model, so mechanistic model simulations were performed to verify the results (Table S4). The results of the model calculations confirm their high agreement; out of 72 cases, identical results were obtained in 68 cases. The calculations performed (variant I, II, III)

https://doi.org/10.5194/hess-2023-63
Preprint. Discussion started: 11 April 2023

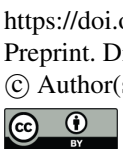

Hydrology and Earth System Sciences
Discussions

for the sub-catchment showed a greater influence of changes in terrain retention and channel capacity on the sensitivity coefficients than the probability of specific flood volume (Fig. 6). For catchments J, S, a 10% decrease in Imp (variant I) increased S_β by 7.55 times and 17.50 times (Fig. 6a, 6d). For variant II (increasing catchment retention), sensitivity coefficients were found to be higher than 51% (catchment S) and 59% (catchment J) compared to variant I, and the highest S_β was obtained in variant III. The S_β values for sub-catchment S are higher than in catchment J by 20.7 times, 19.3 times and 14.7 times for variants I, II and III, respectively. These results provide relevant information for planning retention infrastructure that reduces outflow.

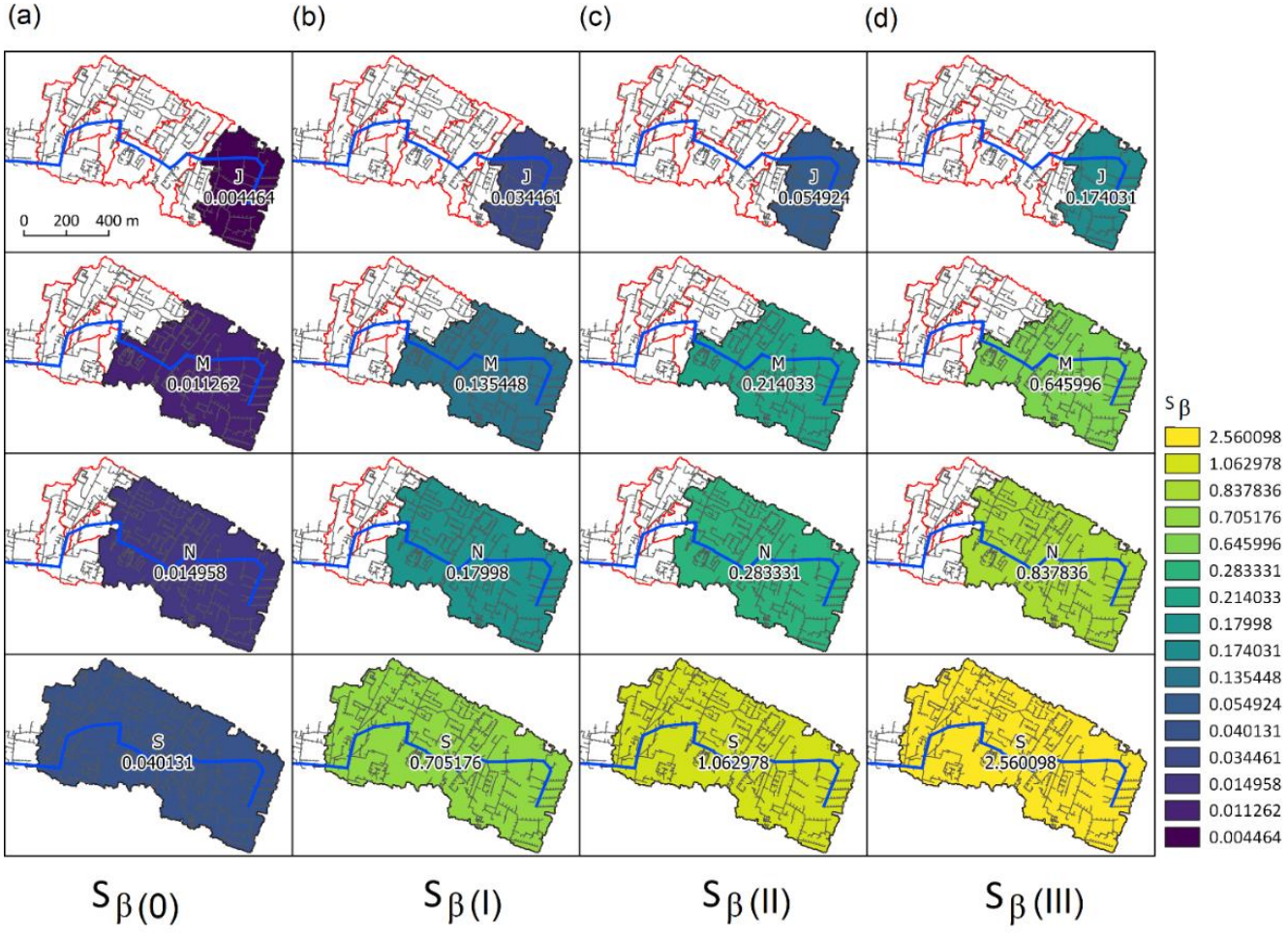

Figure 6. Sensitivity coefficient (S_β) in sub-catchments for: (a) present state (0) and for (b) I, (c) II, (d) III corrective action variants.

4.7. Probability of failure (module 9)

Based on SWMM model parameters determined via the MCM method (Table S1), probability of failure (p_F) was computed for convection rainfall in Kielce with a duration time of t_r=30 min and P_{tot}= 9.61 mm. The following threshold values

https://doi.org/10.5194/hess-2023-63
Preprint. Discussion started: 11 April 2023

Hydrology and Earth System Sciences
Discussions
Open Access
EGU

of $n_{sew(m)}$ were adopted for calculations: $n_{sew(m)}$ = 0.015 – 0.045 $m^{-1/3}$·s, coupled with three variants of catchment characteristics: Imp = 0.36 and Impd =0.40; Imp = 0.35 and Impd = 0.40; Imp = 0.35 and Impd = 0.42. The impact of canal retention (Vk = 750, 850, 950 m^3); density of stormwater network (Gk = 0.0075, 0.0080, 0.0085 m·ha^{-1}; Gkd = 0.005, 0.006, 0.007 m·ha^{-1}) in upper and lower part of the catchment on probability of failure (p_F) was also analysed. The Manning roughness coefficients of the channels (n_{sew}) for the analysed variants were presented as empirical distribution (CDF). In Figure 7a, 8a the results for Imp = 0.36, Impd = 0.40 and Vk = 750, 850, 950 m^3 are presented, while other variants are shown in Figures S18, S19.

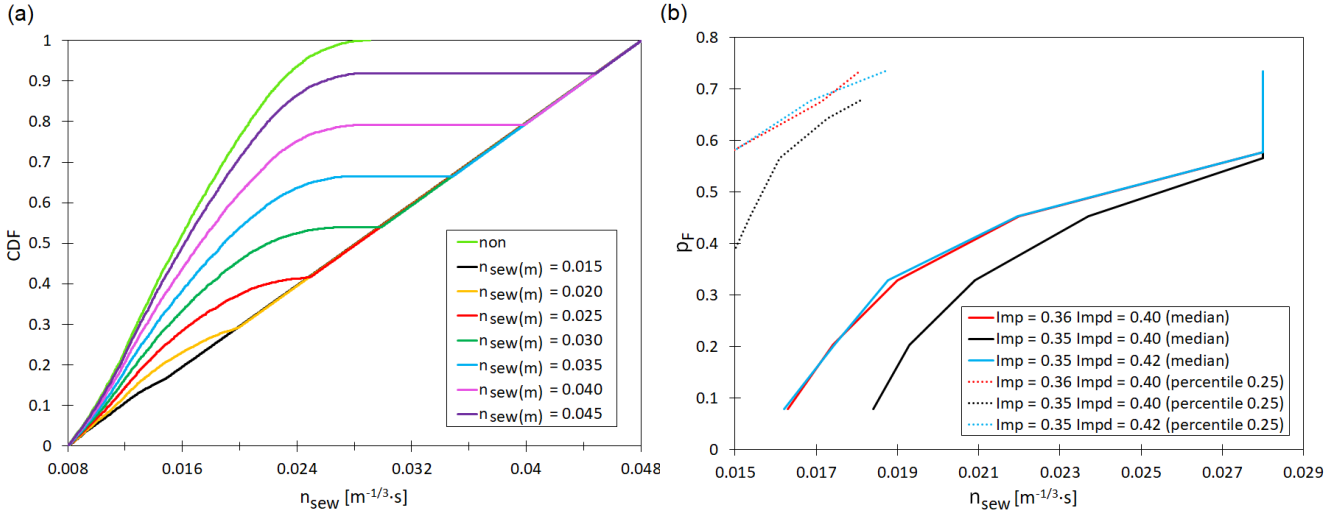

Figure 7. (a) Empirical distributions of threshold values of Manning roughness coefficients of channel (n_{sew}). (b) Impact of Manning roughness coefficient of channel on failure probability (p_F) in relation to Imp, Impd.

Figure 7b presents the impact of n_{sew}=f($n_{sew(m)}$) for percentiles 0.25 and 0.50 (based on the curves in Figures 7b, 8b, 8c, 8d, S25, S26 the values of the respective percentiles for the analysed $n_{sew(m)}$) on the probability of failure (p_F). Assuming that Manning roughness coefficients – $n_{sew(un)}$ determined by MC simulation which exceeds the threshold triggers the corrective actions of sewer pipes resulting in reduction of roughness below $n_{sew(m)}$ following the condition in which the stormwater network functions $p_m = f(X_{rain}, X_{SWMM}, X_{Ctchm}) > 0.75$ for an independent rainfall event, it was found out, that an appropriate decrease of percentiles (0.25 and 0.50 - median) leads to improved network operation and to a lower failure probability (Figures. 7a, 7b). It was observed that the change of percentile 0.50 for n_{sew} for a sample from MC simulation leads to a decrease from 0.028 $m^{-1/3}$·s to 0.021 $m^{-1/3}$·s (as a result of correction $n_{sew(un)} < n_{sew(m)}$) and to improved stormwater network operation understood as a lower probability of failure (decrease of p_F from 0.68 to 0.42 for Imp = 0.36 and Impd = 0.40). These results confirm the significance of catchment characteristics (Imp, Impd) for the operability of a stormwater network. For Impd = 0.40, the reduction in catchment impervious area (Imp) from 0.36 to 0.35, at percentile n_{sew} = 0.019 $m^{-1/3}$·s results in a decrease in failure probability from p_F = 0.42 to p_F = 0.33 (Figure 7b).

Great impact of channel retention (Vk) and density of stormwater network in the upper and lower part of a catchment (Gkd and Gk, respectively) on probability of failure p_F were indicated (Figure 8). For n_{sew} < 0.0215 $m^{-1/3}$·s p_F reached higher

https://doi.org/10.5194/hess-2023-63
Preprint. Discussion started: 11 April 2023

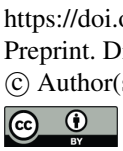

Hydrology and Earth System Sciences
Discussions

values (max. 0.41) than for Vk = 850 m^3 and Vk = 950 m^3. The highest failure probability (p_F = 0.80) was obtained for Vk = 750 m^3 (n_{sew} = 0.031 $m^{-1/3}$·s), while the lowest p_F = 0.65 was obtained for Vk = 950 m^3 (Figure 8b).

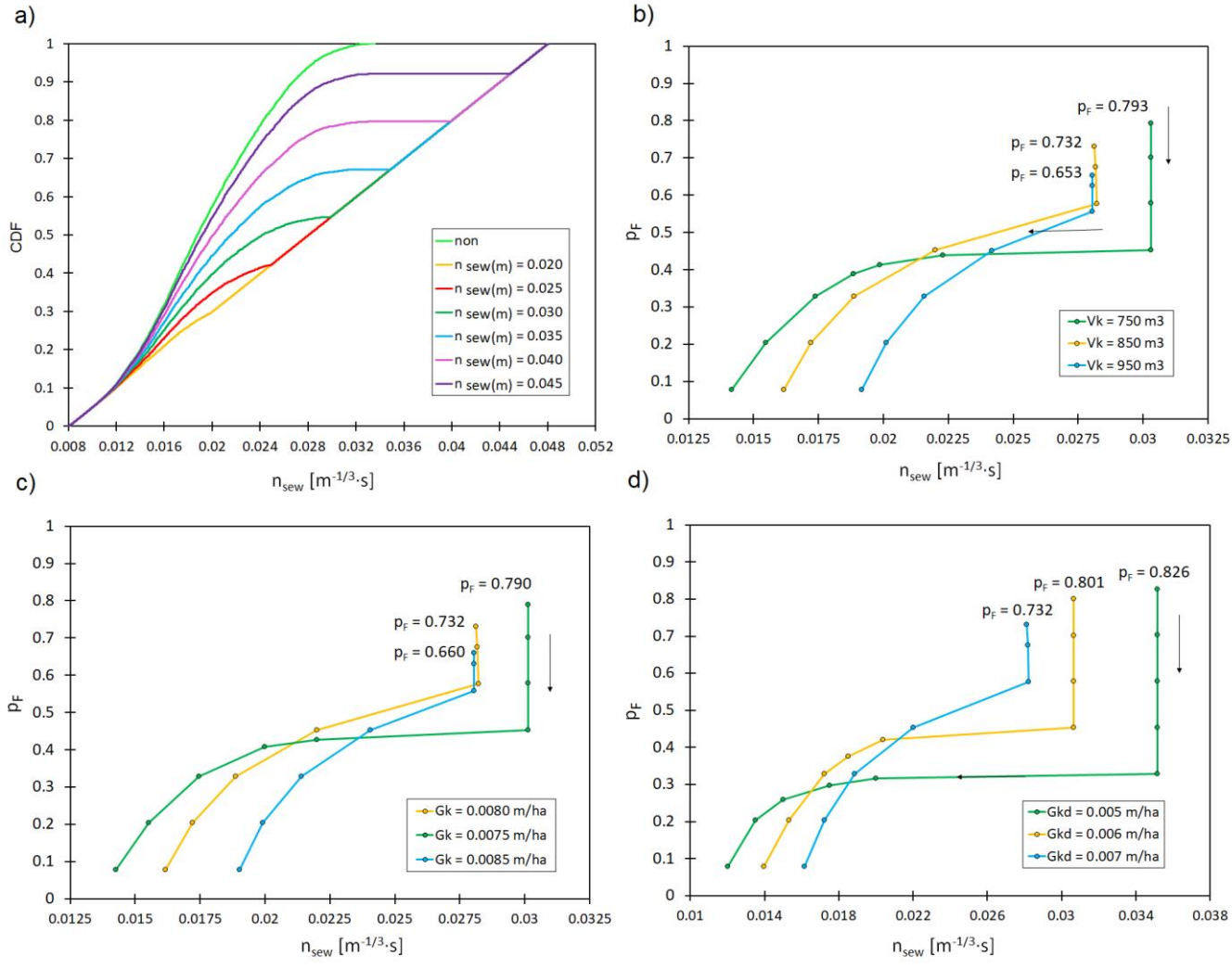

Figure 8. (a) Empirical distributions of threshold values of Manning roughness coefficients of channels (n_{sew}) for Vk = 950m^3. Impact of Manning roughness coefficient for channel on failure probability (p_F) in relation to: (b) Vk – canal retention, (c) Gk - length of stormwater channel per impervious area in a catchment ($m \cdot ha^{-1}$), (d) Gkd - length of a channel per impervious area below closing cross-section ($m\ ha^{-1}$).

Furthermore, the highest probability of failure p_F = 0.79 was obtained for Gk = 0.0075 $m \cdot ha^{-1}$ (n_{sew} = 0.031 $m^{-1/3}$·s), while the lowest for Gk = 0.0085 $m \cdot ha^{-1}$ (n_{sew} = 0.0276 $m^{-1/3}$·s) (Figure 8c). It was established that for n_{sew} < 0.023 $m^{-1/3}$·s computed values of p_F for Gk = 0.0075 $m \cdot ha^{-1}$ and Gk = 0.0080 $m \cdot ha^{-1}$ are higher than 0.41. Moreover, the highest failure probability p_F for n_{sew} = 0.035 $m^{-1/3}$·s was equal to 0.82 for Gkd = 0.005 $m \cdot ha^{-1}$, while for Gkd = 0.007 $m \cdot ha^{-1}$ it was 0.73 (Figure 8d).

https://doi.org/10.5194/hess-2023-63
Preprint. Discussion started: 11 April 2023

Hydrology and Earth System Sciences
Discussions

5. Discussion

Developing and calibrating mathematical models to simulate stormwater network operation under hydraulic overloads is one of the latest areas of research. In comparison to the models used so far (Li and Willems, 2019; Thorndahl 2009), the logistic regression model proposed in this study includes SWMM model parameters describing catchment retention and, at the same time, the characteristics of the catchment and stormwater network (Table 4).

Table. 4. Comparison of developed model for identification of specific flood volume to literature data

Study	Criteria	M	I	R	C	S	P
Duncan et al. (2011)	occurrence of flooding	✓	•	✓	✓	✓	•
Jato - Espino et al. (2018)	occurrence of flooding	✓	✓	✓	✓	✓	•
Jato - Espino et al. (2019)	occurrence of flooding	✓	•	✓	✓	✓	•
Li and Willems (2020)	occurrence flooding	✓	✓	✓	✓	✓	•
Szeląg et al. (2021)	volume	✓	✓	✓	✓	✓	✓
Szeląg et al. (2022a)	occurrence of flooding	•	•	✓	✓	✓	✓
Szeląg et al. (2022b)	specific flood volume	✓	✓	✓	•	•	✓
Thorndahl et al. (2008)	volume	✓	✓	✓	•	✓	✓
Verbovski et al. (2022)	volume	✓	✓	✓	•	•	•
Fu et al. (2011)	volume	•	•	✓	✓	✓	✓
Chen et al. (2020)	volume	•	•	✓	✓	✓	✓
Fraga et al. (2016)	volume	•	•	✓	✓	✓	✓
this study	specific flood volume	✓	✓	✓	✓	✓	✓

where: M (method); the models were divided into two groups: mechanistic (·) and statistical model (∨); R (rainfall); C (catchment); S (sewer); P (calibration parameter); I (interpretation model, based on estimated factors the impact of analysed factors on stormwater flooding can be determined).

Apart from the model developed in this study, the above-mentioned factors are only included in MCM, which have a form of differential equations. Therefore, they require a large number of simulations in order to determine the impact of selected variables on computation results of specific flood volume. Free from such drawbacks are statistical models (Table S4) that take the form of empirical relationships. For models developed with neural networks, there is a need of performing additional analyses (Ke et al, 2020; Yang et al., 2020). Jato – Espino et al. (2018, 2019) and Li and Willems (2020) analysed stormwater flooding from manholes based on catchment characteristics and stormwater network characteristics (Table 4). Szeląg et al. (2022) confirmed their results and developed a model for identification of stormwater flooding in a catchment, but not considered catchment retention. In this context, the approaches cited above were insufficient to analyse the impact of different types of pavement (for example roof, road, parking etc.) on sewage flooding. Fu et al. (2011), Thorndahl et al. (2009), Szeląg et al. (2022b) analysed the uncertainty of the identified parameters, which allowed, for example, to correct for impervious area

https://doi.org/10.5194/hess-2023-63
Preprint. Discussion started: 11 April 2023


Hydrology and Earth System Sciences
Discussions

retention, roughness coefficient without being able to correct for catchment imperviousness, which limited the use of the models in catchment management. The approach proposed in this study is a combination of these two solutions, which provides a tool which can be successfully implemented to manage other catchments.

The results of this study confirmed the major significance and huge interaction between catchment characteristics and SWMM model parameters. This fact can be further compared by several references (Li and Willems, 2020; Jato – Espino et al., 2019; Zhuo et al., 2019) presenting comparisons of flooding simulations in urban catchments. This analysis indicated that an impervious area in a catchment (Imp, Impd) leads to the increase of flooding; reverse dependency was obtained by Jato – Espino et al. (2018) when modelling flooding from manholes. Increase in channel volume above the closing cross-section of a catchment (Vk) and its longitudinal slope (Jkp) results in the decrease of flooding, that was confirmed for Espoo catchment in Finland (Jato – Espino et al. 2018). The increase of unit impervious area per the length of main stormwater interceptor (Gk, Gkd) results in smaller volume of stormwater flooding. This is due to the relationship that the longer the channel, the greater the number of manholes. Huang et al. (2018) based on observations conducted in a complex stormwater system indicated the impact of catchment location and hydrological conditions on the peak flow of flooding. Yao et al. (2019) obtained similar results after computations with a MCM for catchments in Beijing and in Dresden (Reyes – Silva et al. 2020).

Calculation results obtained in this study confirmed relevant impact of rainfall data, catchment characteristics, and stormwater network characteristics on sensitivity coefficients – relationships between SWMM parameters and specific flood volume. For rainfall data and catchment characteristics (assumed as constant) it was proved that correction coefficient of impervious area (β) and the Manning roughness coefficient for channels (n_{sew}) have the greatest impact on specific flood volume. The results of this computations were consistent with Thorndahl et al. (2009), who simulated flooding from a single manhole in the Frejlev catchment (Belgium), based on rainfall data and calibrated parameters of a MCM. These findings were confirmed by calculations Fu et al. (2012) and Prodanovic et al. (2022) respectively for catchments of 400 ha and 8 ha. Szeląg et al. (2021, 2022b) based on simulations with MCM including uncertainty of SWMM parameters proved the key impact of Manning roughness coefficient of sewers on specific flood volume (for rainfall event t_r = 30 min and P_t = 15.25 mm). Fraga et al. (2016) used GLUE+ GSA method for a road catchment and indicated the impact of rainfall data (rainfall duration, depth, temporal distribution) on sensitivity analysis results. It was confirmed in computations of stormwater flooding using logit model (Szeląg et al. 2022) and specific flood volume calculations with SWMM model (Freni et al. 2012). Xing et al. (2021) used MCM to determine characteristics of spatial development and stormwater characteristics in Chongqing catchment (China) on the depth of stormwater flooding. The aforementioned research studies indicate the impact of rainfall data, catchment characteristics, and stormwater network characteristics on sensitivity of hydrodynamic simulation model for stormwater flooding.

The sensitivity analysis development proposed in this study enabled its application for catchments with different characteristics, which is an improvement compared to previously applied, more specified approaches (Cristiano et al. 2019; Fatone et al., 2021). Differences in probability of occurrence/sensitivity coefficients indicate the influence of catchments downstream on conditions in the catchment above. The variation in sensitivity coefficients does not account for local conditions

https://doi.org/10.5194/hess-2023-63
Preprint. Discussion started: 11 April 2023


Hydrology and Earth System Sciences
Discussions

within the side channels. Due to the creation of successive sub-catchments by combining them, the conditions of the sewer system in its area are averaged out, making the interpretation of the results difficult. Using the developed tool, catchment management may become difficult when there is a particularly hydraulically overloaded area within the catchment, which impacts neighbouring sub-catchments.

As in the case to the sensitivity analysis, in this study the extension of the sewer system failure assessment has been adapted to enable the implementation for a random catchment (for the sewer system without pump stations). Calculations outputs showed the influence of the catchment and sewage network characteristics on the failure probability. The introduction of the maximum allowable value of the Manning roughness coefficient for the sewer channel, enabled to model the improvement of the operating conditions of the sewage network under uncertainty. A similar approach was used in the study of Fu et al. (2012) by limiting to probabilistic rainfall characteristics (Del Giudice, et al. 2013) and using a MCM to simulate the drainage system. Fu et al. (2011) modified the above approach by focusing on the impact of uncertainty in the calibrated parameters on flooding; however, it was not possible to analyse retention, channel capacity on system performance.

6. Conclusions

In this study a novel simulator of logistic regression extended by advanced risk assessment was developed for modeling stormwater systems operation under uncertainty. The proposed model is an alternative approach to mechanistic models, that can be used at the preliminary stage of analyses related to spatial planning, urban development and expansion etc. This is of major significance since at the preliminary stage, the data set for building catchment models is limited and urgent demand for simulation algorithm to assist decision making is required. Assuming Manning roughness coefficients – $n_{sew(un)}$ estimations that exceed the threshold triggers corrective actions of sewer pipes resulting in a reduction of roughness below $n_{sew(m)}$ following the condition of proper functioning of the stormwater network ($p_m > p_{mcr}$). Appropriate decrease of percentiles (0.25 and 0.50 - median) led to improved network operation and to a lower failure probability requirement.

In the adopted hydrodynamic model (based LRM), the impact of rainfall data, catchment characteristics (impervious areas in the downstream and upstream) and stormwater network characteristics (the length of channel per unit impervious area, channel slope and volume) as well as SWMM parameters (roughness coefficient for sewer channel, correction coefficient for percentage impervious area Manning roughness coefficients for impervious area) were included simultaneously. The obtained simulations results show the strong interaction between the above-listed parameters. This is extremely relevant in the context of models calibration that can be applied to analyse stormwater network operation and to support the decision-making process (management of stormwater in an urban catchment). Since the proposed solution analyses the spatial distribution of sensitivity coefficients, it is possible to identify the most vulnerable areas inside a catchment that require specific attention while identifying SWMM model parameters, which could also be taken into account when locating measuring facilities.

https://doi.org/10.5194/hess-2023-63
Preprint. Discussion started: 11 April 2023


Hydrology and Earth System Sciences
Discussions

7 Appendices

Appendix A: List of Symbols

Symbols:

A_{imp} – area of impervious surface (ha),

dH1 – height difference of the terrain at section above closing cross-section (m),

dHp – height difference at section above closing cross-section (m),

CDF – Cumulative Distribution Function (–),

d_{imp} – retention depth of impervious areas (mm),

d_{perv} – retention depth of pervious areas (mm),

F – catchment surface area (ha),

Gk – length of stormwater channel per impervious area in a catchment ($m \cdot ha^{-1}$),

Gkd – length of a channel per impervious area below closing cross-section ($m \cdot ha^{-1}$),

GLUE - Generalized Likelihood Uncertainty Estimation,

Hst – the height of a manhole at closing cross-section (m),

Imp – impervious area,

Impd – impervious area of a catchment of downstream area,

J – average rainfall intensity ($l \cdot (s \cdot ha)^{-1}$),

Jkp – channel slope above closing cross-section of a catchment

K – total number of sewer manholes (–),

Lk – length of channel above closing cross-section of a catchment (m),

L(Q/θ) – likelihood function,

n_{imp} – Manning roughness coefficient for impervious areas ($m^{-1/3} \cdot s$),

n_{perv} – Manning roughness coefficient for pervious areas ($m^{-1/3} \cdot s$),

n_{sew} – Manning roughness coefficients of sewer channels ($m^{-1/3} \cdot s$),

Q_z – denote *z*-th value from the times series of observed and computed discharges ($m^3 \cdot s^{-1}$),

P_t – maximum depth of rainfall (mm),

p – cumulative distribution function (CDF),

p_m – probability of specific flood volume,

P(θ) – stands for *a priori* parameter distribution,

R.t. – height difference of the channel (m),

S_{xi} – sensitivity coefficient,

x_i – independent variables,

SWMM – Storm Water Management Model,

https://doi.org/10.5194/hess-2023-63
Preprint. Discussion started: 11 April 2023


Hydrology and Earth System Sciences
Discussions

t_r – duration of rainfall (min),

V () – variance,

Vk – volume of stormwater channel (m^3),

Vkd – total retention of a catchment.

Vkp – volume of the channel above the closing cross-section of a catchment (m^3),

Vrd – catchment retention above the closing cross-section (m^3),

$V_{t(i)}$ – floodings volume from i - th sewer manhole (where: i = 1, 2, 3, …, k) (m^3),

W – width of the runoff path in a subcatchment (m),

α – Coefficient for flow path width (–),

β – Correction coefficient for percentage of impervious areas (–),

γ – Correction coefficient for subcatchment slope (–),

ε- a scaling factor for the variance of model residua, used to adjust the width of the confidence intervals,

κ – specific flood volume ($m^3 \cdot ha^{-1}$),

Code availability: The authors announce that there is no problem sharing the used model and codes upon request to the corresponding author.

Data availability: The authors confirm that data supporting the findings of this study are available from the corresponding author upon request.

Author contribution: Conceptualization: Szeląg, Methodology: Fatone, Szeląg, Kiczko; Formal analysis and investigation: Szeląg, Kiczko, Stachura, Wałek; Writing - original draft preparation: Szeląg, Kowal, McGarity, Wojciechowska, Wałek, Fatone, Caradot; Writing - review and editing: Kowal, Wojciechowska, McGarity, Fatone, Caradot; Supervision: Szeląg, Kowal, McGarity, Wojciechowska, Caradot.

Competing interests: The authors declare that they have no conflicts of interest.

References

Babovic, F., Mijic, A., Madani, K.: Decision making under deep uncertainty for adapting urban drainage systems to change. Urban Water J, 15, 552 – 560. https://doi.org/10.1080/1573062X.2018.1529803, 2018.

Ball, J., E. : An Assessment of Continuous Modeling for Robust Design Flood Estimation in Urban Environments. Front. Earth Sci. 8, 1 – 10. http://doi.org/10.3389/feart.2020.00124, 2020.

Beven, K., Binley, A.: The future of distributed models: model calibration and uncertainty prediction, Hydrol. Process., 6, 279-298, https://doi.org/10.1002/hyp.3360060305, 1992.

Bui, D.T., Hoang, N.D., Martínez-Álvarez, F., Ngo, P.T. T., Hoa, P.V., Pham, T.D., Samui, P., Costache, R.: A novel deep learning neural network approach for predicting flash flood susceptibility: A case study at a high frequency tropical storm area, Sci. Total Environ, 701, 134413. https://doi.org/10.1016/j.scitotenv.2019.134413, 2018.

653 Cea, L., Costabile, P.: Flood Risk in Urban Areas: Modelling, Management and Adaptation to Climate Change. A Review.
654 Hydrology, 9, 50. https://doi.org/10.3390/ hydrology9030050, 2022.
655 Chang, H., Pallathadka, A., Sauer, J., Grimm, N.B., Zimmerman, R., Cheng, C., Iwaniec, D.M., Kim, Y., Lloyd, R.,
656 McPhearson, T., Rosenzweig, B., Troxler, T., Welty, C., Brenner, R., Herreros-Cantis, P.: Assessment of urban flood
657 vulnerability using the social-ecological-technological systems framework in six US cities, Sustain. Cities Soc. 68, 102786,
658 https://doi.org/10.1016/j.scs.2021.102786, 2020.
659 Chen, L., Li, S., Zhong, Y., and Shen, Z.: Improvement of model evaluation by incorporating prediction and measurement
660 uncertainty, Hydrol. Earth Syst. Sci., 22, 4145–4154, https://doi.org/10.5194/hess-22-4145-2018, 2018.
661 Chen,W., Li, Y., Xue, W., Shahabi, H., Li, S., Hong, H., Wang, X., Bian, H., Zhang, S., Pradhan, B., Bin Ahmad, B.: Modeling
662 flood susceptibility using data-driven approaches of naïve Bayes tree, alternating decision tree, and random forest methods,
663 Sci. Total Environ. 701, 134979. https:// doi.org/10.1016/j.scitotenv.2019.134979, 2019.
664 Cristiano, E., ten Veldhuis, M. C., Wright, D. B., Smith, J. A., and van de Giesen, N.: The Influence of Rainfall and Catchment
665 Critical Scales on Urban Hydrological Response Sensitivity, Water Resour. Res., 55, 3375–3390,
666 https://doi.org/10.1029/2018WR024143, 2019.
667 Dotto, C. B. S., Kleidorfer, M., Deletic, A., Rauch, W., and McCarthy, D. T.: Impacts of measured data uncertainty on urban
668 stormwater models, J. Hydrol., 508, 28-42, https://doi.org/10.1016/j.jhydrol.2013.10.025, 2014.
669 DWA-A118E: Hydraulic Dimensioning and Verification of Drain and Sewer Systems. Ger. Assoc. Water Wastewater Waste,
670 2006.
671 Fatone, F., Szeląg, B., Kiczko, A., Majerek, D., Majewska, M., Drewnowski, J., and Łagód, G.: Advanced sensitivity analysis
672 of the impact of the temporal distribution and intensity of rainfall on hydrograph parameters in urban catchments, Hydrol.
673 Earth Syst. Sci., 25, 5493–5516, https://doi.org/10.5194/hess-25-5493-2021, 2021.
674 Fong, T. and Chui, M.: Modeling and interpreting hydrological responses of sustainable urban drainage systems with
675 explainable machine learning methods, Hydrol. Earth Syst. Sci., 25, 5839 – 5858. https://doi.org/10.5194/hess-2020-460,
676 2020.
677 Fraga, I., Cea, L., Puertas, J., Suárez, J., Jiménez, V., Jácome, A.: Global sensitivity and GLUE-based uncertainty analysis of
678 a 2D-1D dual urban drainage model, J Hydrol Eng., 21, 04016004, https://doi.org/10.1061/(ASCE)HE.1943-5584.0001335,
679 2016.
680 Fu, G., Butler, D., Khu, S-T., Sun, S.: Imprecise probabilistic evaluation of sewer flooding in urban drainage systems using
681 random set theory, Water Resour Res, 47. https://doi.org/10.1029/2009WR008944, 2011.
682 Fu, G., Butler, D.: Copula-based frequency analysis of overflow and flooding in urban drainage systems, J. Hydrol., 510, 49–
683 58, https://doi.org/10.1016/j.jhydrol.2013.12.006, 2014.
684 Guo, K., Guan, M., Yu, D.: Urban surface water flood modelling – a comprehensive review of current models and future
685 challenges. Hydrol. Earth Syst. Sci., 25, 2843–2860. https://doi.org/10.5194/hess-25-2843-2021, 2021.
686 Harrell, F.E.: Regression Modeling Strategies: With Applications to Linear Models, Logistic Regression, and Survival

687 Analysis. Springer Series in Statistics, New York. ISBN: 9781475734621, 2001.
688 Hettiarachchi, S., Wasko, C., Sharma, A. : Increase in flood risk resulting from climate change in a developed urban watershed
689 – the role of storm temporal patterns. Hydrol. Earth Syst. Sci., 22, 2041–2056. https://doi.org/10.5194/hess-22-2041-2018,
690 2018.
691 Hung, W., Hobbs, F. B.: How can learning-by-doing improve decisions in stormwater management? A Bayesian-based
692 optimization model for planning urban green infrastructure investments. Environ Modell Softw, 113, 59 – 72.
693 https://doi.org/10.1016/j.envsoft.2018.12.005, 2019.
694 Jato-Espino, D., Sillanpää, N., Andrés-Doménech, I., Rodriguez-Hernandez, J.: Flood Risk Assessment in Urban Catchments
695 Using Multiple Regression Analysis, J. Water Resour. Plan. Manag., 144, 04017085, https://doi.org/10.1061/(asce)wr.1943-
696 5452.0000874, 2018.
697 Jiang, Y., Zevenbergen, C., Mab, Y.: Urban pluvial flooding and stormwater management: A contemporary review of China's
698 challenges and "sponge cities" strategy, Environ Sci Policy. 80, 132 – 143. https://doi.org/10.1016/j.envsci.2017.11.016, 2018.
699 Karamouz M, and Nazif S (2013). "Reliability-based flood management in urban watersheds considering climate change
700 impacts." J. Water Resour. Plann. Manage, http://doi.org/10.1061/(ASCE)WR.1943-5452.0000345, 520–533.
701 Ke, Q., Bricker, J., Tian, Z., Guan, G., Cai, H., Huang, X., Yang, H., Liu, J.: Urban pluvial flooding prediction by machine
702 learning approaches – a case study of Shenzen city, China, Adv. Water Resour., 145, 103719,
703 http://doi.org/10.1016/j.advwatres.2020.103719, 2020.
704 Kelleher, C., McGlynn, B., and Wagener, T.: Characterizing and reducing equifinality by constraining a distributed catchment
705 model with regional signatures, local observations, and process understanding, Hydrol. Earth Syst. Sci., 21, 3325– 3352,
706 https://doi.org/10.5194/hess-21-3325-2017, 2017.
707 Khan, M.P., Hubacek, K., Brubaker, K.L., Sun, L., Moglen, G.E. : Stormwater Management Adaptation Pathways under
708 Climate Change and Urbanization. J. Sustainable Water Built Environ, 8, 04022009.
709 https://doi.org/10.1061/JSWBAY.0000992, 2022.
710 Kiczko, A., Szeląg, B., Kozioł, A.P., Krukowski, M., Kubrak, E., Kubrak, J., Romanowicz, R.J.: Optimal capacity of a
711 stormwater reservoir for flood peak reduction, J. Hydrol. Eng., 23:04018008, https://doi.org/10.1061/(ASCE)HE.1943-
712 5584.0001636, 2018.
713 Kim, Y., Eisenberg, D.A., Bondank, E,N., Chester, M.V., Mascaro, G., Underwood, S.: Fail-safe and safe-to-fail adaptation:
714 decision-making for urban flooding under climate change. Clim Change, 145, 397 – 412. https://doi.org/10.1007/s10584-017-
715 2090-1, 2015.
716 Kirshen, P., Caputo, L., Vogel, R.M., Mathisen, P., Rosner, A., Renaud, T.: Adapting urban infrastructure to climate change:
717 a drainage case study, J. Water Resour. Plan. Manag., 141, 04014064, https://doi.org/10.1061/(ASCE)WR.1943-5452.0000443,
718 2015.
719 Knighton, J., Lennon, E., Bastidas, L., White, E.: Stormwater detention system parameter sensitivity and uncertainty analysis
720 using SWMM, J. Hydrol. Eng., 21, 05016014, https://doi.org/10.1061/(ASCE)HE.1943-5584.0001382, 2016.

721 Kobarfard, M., Fazloula, R., Zarghami M., Akbarpour: Evaluating the uncertainty of urban flood model using glue approach.
722 Urban Water J, 19, 600 – 615. https://doi.org/10.1080/1573062X.2022.2053865, 2022.
723 Lei, X., Chen, W., Panahi, M., Falah, F., Rahmati, O., Uuemaa, E., Kalantari, Z., Ferreira, C.S.S., Rezaie, F., Tiefenbacher,
724 J.P., Lee, S., Bian, H.: Urban flood modeling using deep-learning approaches in Seoul, South Korea. J Hydrol, 601, 126684.
725 https://doi.org/10.1016/j.jhydrol.2021.126684, 2021.
726 Li, X., Willems, P.: A Hybrid Model for Fast and Probabilistic Urban Pluvial Flood Prediction, Water Resour. Res., 56,
727 e2019WR025128, https://doi.org/10.1029/2019WR025128, 2020.
728 Ma, B., Wu, Z., Hu, C., Wang, H., Xu, H., Yan, D., Soomro, S. : Process-oriented SWMM real-time correction and urban
729 flood dynamic simulation. J Hydrol, 605, 127269. https://doi.org/10.1016/j.jhydrol.2021.127269, 2022.
730 Martins, R., Leandro, J., Djordjevi´c, S.: Influence of sewer network models on urban flood damage assessment based on
731 coupled 1D/2D models. J. Flood Risk Manag. 11, 717 – 728. https://doi.org/10.1111/jfr3.1224, 2018.
732 Mignot, E., Li, X., Dewals, B.: Experimental modelling of urban flooding: A review, J. Hydrol., 568, 334-342.
733 https://doi.org/10.1016/j.jhydrol.2018.11.001, 2019.
734 Miller, J., Kim, H., Kjeldsen, T.R., Packman, J., Grebby, S., Dearden, R.: Assessing the impact of urbanization on storm runoff
735 in a peri-urban catchment using historical change in impervious cover. J Hydrol, 515, 59 – 70.
736 https://doi.org/10.1016/j.jhydrol.2014.04.011, 2014.
737 Morio, J.: Global and local sensitivity analysis methods for a physical system, Eur. J. Phys., 32, 1577–1583,
738 https://doi.org/10.1088/0143-0807/32/6/011, 2011.
739 Razavi, S., Gupta, H.V.: A multi – method Generalized Global Sensitivity Matrix approach to accounting for the dynamical
740 nature of earth and environmental systems models, Environ. Model. Softw., 114, 1 – 11.
741 https://doi.org/10.1016/j.envsoft.2018.12.002, 2019.
742 Romanowicz, R.J., Beven, K.J.: Comments on generalised likelihood uncertainty estimation, Reliab. Eng. Syst. Saf., 91, 1315–
743 1321, https://doi.org/10.1016/j.ress.2005.11.030, 2006.
744 Rosenzweig, B.R., Cantis, H., Kim, Y., Cohn, A., Grove, K., Brock, J., Yesuf, J., Mistry, P., Welty, C., McPhearson, T., Sauer,
745 J., Chang, H: The value of urban flood modeling. Earth's Future, 9, e2020EF001739. https://doi. org/10.1029/2020EF00173,
746 2021.
747 Shafizadeh-Moghadam, H., Valavi, R., Shahabi, H., Chapi, K., Shirzadi, A.:. Novel forecasting approaches using combination
748 of machine learning and statistical models for flood susceptibility mapping. J Environ Manage, 217, 1 – 11.
749 https://doi.org/10.1016/j.jenvman.2018.03.089, 2018.
750 Shrestha, A., Mascaro, G., Garcia, M.: Effects of stormwater infrastructure data completeness and model resolution on urban
751 flood modeling. J Hydrol, 607, 127498. https://doi.org/10.1016/j.jhydrol.2022.127498, 2022.
752 Siekmann, M., Vomberg, N., Mirgartz, M., Pinnekamp, J., Mühle, S. : Multifunctional Land use in Urban Spaces to Adapt
753 Urban Infrastructure, 611 – 625. In: Climate Change and the Sustainable Use of Water Resources, 2011.
754 Siekmann, M., Pinnekamp, J.: Indicator based strategy to adapt urban drainage systems in regard to the consequences caused

by climate change, in: 12th International Conference on Urban Drainage. pp. 11–16., 2011.

Sonavane N., Rangari, V.A., Waikar, M.L., Patil, M.: Urban storm-water modeling using EPA SWMM – a case study of Pune city. 2020 IEEE Bangalore Humanitarian Technology Conference (B-HTC). 10.1109/B-HTC50970.2020.9297900, 2020.

Sun, Y., Liu, Ch., Du, X., Yang, F., Yao, Y., Soomro, S., Hu, C.: Urban storm flood simulation using improved SWMM based on K-means clustering of parameter samples. J Flood Risk Manag. e12826. https://doi.org/10.1111/jfr3.12826, 2022.

Szelag, B., Suligowski, R., Drewnowski, J., De Paola, F., Fernandez – Morales, F.J., Bąk, Ł.: Simulation of the number of storm overflows considering changes in precipitation dynamics and the urbanisation of the catchment area: A probabilistic approach, J. Hydrol., 598, 126275, https://doi.org/10.1016/j.jhydrol.2021.126275, 2021b.

Szeląg, B., Kiczko, A., Łagód, G., De Paola, F.: Relationship between rainfall duration and sewer system performance measures within the context of uncertainty, Water Res Manage., 35, 5073 – 5087, https://doi.org/10.1007/s11269-021-02998-x, 2021.

Szeląg, B., Suligowski, R., De Paola, F., Siwicki, P., Majerek, D., Łagód, G.: Influence of urban catchment characteristics and rainfall origins on the phenomenon of stormwater flooding: Case study, Environ. Model. Softw., 150, 105335, https://doi.org/10.1016/ j.envsoft.2022.105335, 2022a.

Szeląg, B., Majerek, D., Kiczko, A., Łagód, G., Fatone, F., McGarity, A.: Analysis of sewer network performance in context of modernization: modeling, sensitivity, uncertainty analysis. 12, 148. http.//doi.org/10.1061/(ASCE)WR.1943 – 5452.0001610.

Taromideh, F., Fazloula, R., Choubin, B., Emadi, A., Berndtsson, R.: Urban Flood-Risk Assessment: Integration of Decision-Making and Machine Learning. Sustainability, 14, 4483. https://doi.org/10.3390/su14084483, 2022.

Thorndahl, S.: Stochastic long term modelling of a drainage system with estimation of return period uncertainty, Water Sci Technol., 59, 2331–2339, https://doi.org/10.2166/wst.2009.305, 2009.

Ursino, N.: Reliability analysis of sustainable storm water drainage systems. WIT Transactions on The Built Environment, 139, 149 – 157. https://doi.org/10.2495/UW140131, 2014.

Yang, Y., Chui, T.F.M.: Modeling and interpreting hydrological responses of sustainable urban drainage systems with explainable machine learning methods, Hydrol. Earth Syst. Sci., 25, 5839–5858, https://doi.org/10.5194/hess-25-5839-2021, 2020.

Yang, Q., Ma, Z., Zhang, S.: Urban Pluvial Flood Modeling by Coupling Raster-Based Two-Dimensional Hydrodynamic Model and SWMM. Water, 14, 1760. https://doi.org/10.3390/ w14111760, 2022.

Wałek, G.: Wpływ dróg na kształtowanie spływu powierzchniowego w obszarze zurbanizowanym na przykładzie zlewni rzeki Silnicy w Kielcach. Jan Kochanowski University Press, Kielce (in Polish), 2019.

Wu, J.Y., Thompson, J.R., Kolka, R.K., Franz, K.J., Stewart, T.W.: Using the Storm Water Management Model to predict urban headwater stream hydrological response to climate and land cover change. Hydrol. Earth Syst. Sci., 17, 4743–4758, https://doi.org/10.5194/hess-17-4743-2013, 2013.

Venvik, G., Bang – Kittilsen, A., Boogaard, F. C.: Risk assessment for areas prone to flooding and subsidence: a case study

https://doi.org/10.5194/hess-2023-63
Preprint. Discussion started: 11 April 2023

Hydrology and Earth System Sciences
Discussions

789 from Bergen, Western Norway. Hydrology Research, 51, 322 – 338. https://doi.org/10.2166/nh.2019.030, 2021.

790 Zhang, W., and Li, T.: The influence of objective function and acceptability threshold on uncertainty assessment of an urban
791 drainage hydraulic model with generalized likelihood uncertainty estimation methodology, Water Resour. Manag., 29, 2059-
792 2072, https://doi.org/10.1007/s11269-015-0928-8, 2015.

793 Zhou, Y., Shen, D., Huang, N., Guo, Y., Zhang, T., Zhang, Y.: Urban flood risk assessment using storm characteristic
794 parameters sensitive to catchment-specific drainage system. Sci. Total Environ. 659, 1362–1369.
795 https://doi.org/10.1016/j.scitotenv.2019.01.004, 2019.
796